GEOPHYSICAL RESEARCH LETTERS, VOL. 35, L20302, doi:10.1029/2008GL035458, 2008

Automated detection and location of Cascadia tremor

Aaron G. Wech[1] and Kenneth C. Creager[1]

Received 24 July 2008; revised 9 September 2008; accepted 12 September 2008; published 17 October 2008.

[1] A new autonomous seismic location and detection methodology enables real-time opportunities for high-resolution spatio-temporal monitoring of non-volcanic tremor. Combining a unique cross-correlation technique with epicenter clustering analysis in northern Cascadia automatically yields thousands of tremor epicenters from the May 2008 Episodic Tremor and Slip (ETS) event while routinely detecting and locating inconspicuous inter-ETS tremor bursts. Although ETS events in this area produce about two weeks of continuous tremor, we find a nearly equal amount of tremor during the last 15-month inter-ETS period. The resulting ETS and inter-ETS epicenters occur in the slow slip region where the plate interface is 30–45 km deep and have a sharp, well-resolved updip boundary about 75 km east of the downdip edge of the seismogenic megathrust zone. This ability to track tremor with high spatio-temporal resolution facilitates automatic tremor monitoring and the mapping of the transition zone and regions of locked zone stress accumulation. **Citation:** Wech, A. G., and K. C. Creager (2008), Automated detection and location of Cascadia tremor, *Geophys. Res. Lett.*, *35*, L20302, doi:10.1029/2008GL035458.

1. Introduction

[2] Improving observations of the periodic phenomenon of Episodic Tremor and Slip (ETS) from the similar subduction zones of southwest Japan and northern Cascadia is bringing the tremor source process into focus. In addition to the spatio-temporal correlation between tremor and slow slip [*Obara et al.*, 2004; *Rogers and Dragert*, 2003], evidence from low-frequency earthquakes comprising tremor in Japan [*Shelly et al.*, 2007] and polarization analysis of tremor in Cascadia [*Wech and Creager*, 2007] suggests tremor and slow slip are manifestations of the same shear process. As this distinction between tremor and slow slip narrows, monitoring when, where and how much tremor occurs becomes increasingly important. These basic observations are critical for better understanding the phenomenon of tectonic tremor and accurately assessing seismic hazards.

[3] From a hazards perspective, near-real time tremor detection and location may serve in forecasting the threat of a megathrust earthquake [*Rogers and Dragert*, 2003] by inferring the temporal and spatial extent of the possible loading of the seismogenic zone. Furthermore, precise estimations of tremor epicenters could facilitate better location estimates of the freely slipping, transition, and locked segments of the subducting Juan de Fuca plate relative to the dense urban centers along the fault margin.

[4] Scientifically, the need for detection and location is fundamental to the evaluation of the role of tremor in subduction zone dynamics. Our understanding of the tremor source process is improving, but there are many first-order questions that a detailed tremor catalog would address: What fraction of total tremor energy is released during an ETS event compared with inter-ETS tremor activity? How does tremor from each ETS and inter-ETS event differ in duration, spatial distribution and migration? How do ETS events nucleate and grow?

[5] In this paper we introduce an automated algorithm that reverses the order of standard detection and location methodology by employing a unique cross-correlation method to generate potential epicenters before using the resulting epicenters to detect tremor. This method simultaneously locates and obviates the labor-intensive human efforts in detecting tremor. When applied over a period of 17 months, we obtain thousands of tremor locations from and between the January 2007 and May 2008 ETS events, providing high-resolution epicentral tracking in space and time while revealing a critical role of inter-ETS tremor in Cascadia subduction zone dynamics.

2. Location Method

[6] Locations are estimated with a cross-correlation method that maximizes tremor signal coherency among seismic stations. Using only near-real-time data from Pacific Northwest Seismic Network (PNSN), Pacific Geoscience Centre (PGC), and EarthScope/Plate Boundary Observatory (PBO) borehole seismometers, we choose a subnet comprising about 20 stations in western Washington and southern Vancouver Island based on geographic distribution and tremor signal-to-noise ratios. For a given 5-minute time window of vertical-component short-period data, we band-pass filter from 1–8 Hz, create envelope functions, low-pass filter at 0.1 Hz, and decimate to 1 Hz.

[7] We obtain centroid location estimates by cross-correlating all station pairs and performing a 3-D grid search over potential source-location S-wave lag times that optimize the cross correlations. This optimization problem is performed once on a 0.1 degree epicenter and 10 km depth grid before reiterating on a finer 0.01 epicenter and 2 km depth grid. The objective function $M(x^{\text{grid}})$ is a weighted L1 norm on all pairs of cross correlograms (equation (1)).

$$M\left(x^{\text{grid}}\right) = \sum_{i=1}^{N} \sum_{j=i+1}^{N} \frac{C_{ij}^{\max} - C_{ij}\left(\delta t_{ij}\left(x^{\text{grid}}\right)\right)}{\Delta C\left(C_{ij}^{\max}\right)} \tag{1}$$

where x^{grid} is a target source position, C_{ij} is the normalized cross correlogram between the ith and jth envelope

[1]Department of Earth and Space Sciences, University of Washington, Seattle, Washington, USA.

0094-8276/08/2008GL035458$05.00

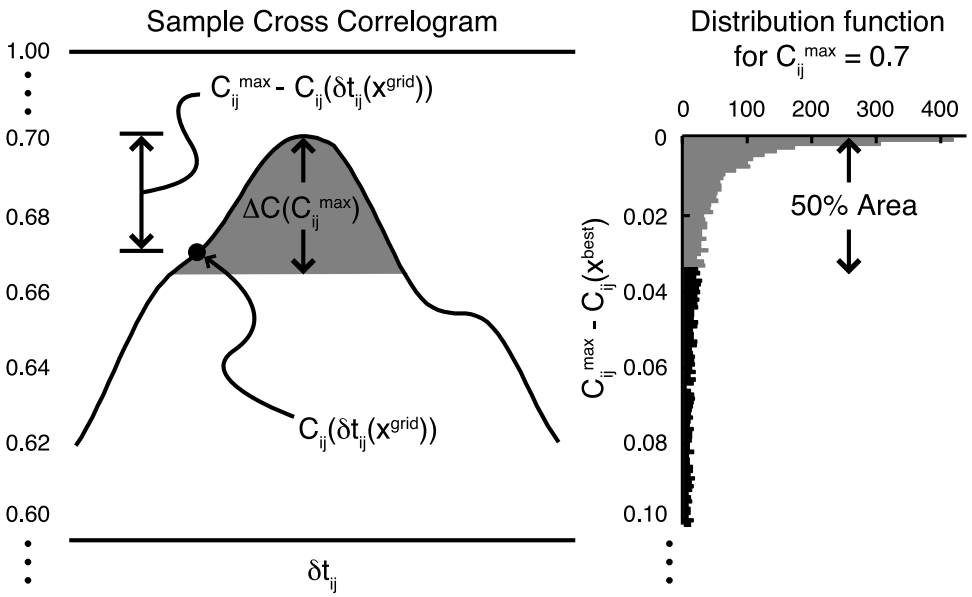

Figure 1. (left) Location method and (right) weighting scheme. Normalized cross correlogram (solid curve, left) between the envelopes for stations i and j as a function of lag time δt evaluated at the differential S-wave travel time $\delta t_{ij}(x^{grid})$ predicted for the 3-D grid location (x^{grid}) to obtain the value $C_{ij}(\delta t_{ij}(x^{grid}))$ (solid black circle). We minimize the vertical correlation distance by minimizing the sum over station pairs of C_{ij}^{max} - $C_{ij}(\delta t_{ij}(x^{grid}))$ inversely weighted by its uncertainty $\Delta C(C_{ij}^{max})$. This uncertainty is assumed to depend only on C_{ij}^{max} and is estimated by the half width of its distribution function. An example distribution function from the best locations of many tremor and non-tremor time windows for $C_{ij}^{max} = 0.7$ is shown in Figure 1 (right) with the half width measurement in gray. This width then defines the error, $\Delta C(C_{ij}^{max})$, (gray, Figure 1 (left)) for all correlograms with $C_{ij}^{max} = 0.7$.

functions, N is the number of seismograms, C_{ij}^{max} is the maximum value of the cross correlogram, and $\delta t_{ij}(x^{grid}) = t_i(x^{grid}) - t_j(x^{grid})$ is the predicted differential S-wave travel time between the ith and jth station using the standard PNSN Puget Sound "P2" model. Thus, for each possible grid location, we predict the lag time, $\delta t_{ij}(x^{grid})$, between station pairs and evaluate its corresponding correlation value from the cross correlogram $C_{ij}(\delta t_{ij}(x^{grid}))$ (Figure 1). While traditional methods seek the source location that minimizes the horizontal time difference between predicted travel time and peak lag time, we seek to minimize the vertical correlation distance between the peak, C_{ij}^{max}, and the predicted correlation, $C_{ij}(\delta t_{ij}(x^{grid}))$. Using only those observations with $C_{ij}^{max} > 0.5$, we maximize network coherency with respect to variations in x^{grid}, by minimizing the sum over station pairs of this vertical correlation distance, C_{ij}^{max} - $C_{ij}(\delta t_{ij}(x^{grid}))$ (Figure 1) inversely weighted by the uncertainty $\Delta C(C_{ij}^{max})$.

3. Weight and Uncertainties

[8] Standard cross-correlation methodology determines relative delay times between stations and uses the resulting differential times and their uncertainties as constraints on source location parameters [e.g., *Obara*, 2002]. Our method differs in that we consider the correlation function itself, not the delay time, to be the raw data, and define misfit to be C_{ij}^{max}-$C_{ij}(x^{best})$. The uncertainty for each observation is assumed to depend only on C_{ij}^{max} and is estimated by the half width of its sample distribution function. This function is determined for each C_{ij}^{max} by finding the "best" source location x^{best} for each 5-minute time window during a 2 week period and storing all values of C_{ij}^{max} and C_{ij}^{max}-$C_{ij}(x^{best})$ for all station pairs regardless of tremor activity (Figure 1). The resulting half-widths of each error distribution (Figure 1) decrease systematically with increasing C_{ij}^{max} and can be described by a polynomial (equation (2)).

$$\Delta C\left(C_{ij}^{max}\right) = 4.97\left(C_{ij}^{max}\right)^4 - 18.94\left(C_{ij}^{max}\right)^3 + 26.73\left(C_{ij}^{max}\right)^2 - 16.59\,C_{ij}^{max} + 3.84. \quad (2)$$

[9] We obtain location uncertainty estimates based on bootstrap [*Efron*, 1979] location reliability. For each time window we randomly remove 10% of the cross-correlograms and search for a location. This step is iterated generating 10 locations for each time window. We interpret the median of the resulting cloud of locations as the source centroid epicenter with an error estimated by the absolute deviation. We tested this scheme against the entire P, S, and coda wave trains of 151 local earthquakes. This test found that 70% of the 133 earthquakes with epicentral error estimates under 5 km lay within 8 km of their network-determined epicentres. The median epicentral difference is 5 km.

4. Detection

[10] The canonical approach to locating tremor begins with tremor detection. Once identified, tremor can be located via cross-correlation [*Obara*, 2002], source scanning [*Kao and Shan*, 2004], picking envelope functions [*McCausland et al.*, 2005], or using slowness observed at small-aperture arrays [*McCausland*, 2006; *La Rocca*, 2008]. Our approach, however, is reversed. We automatically

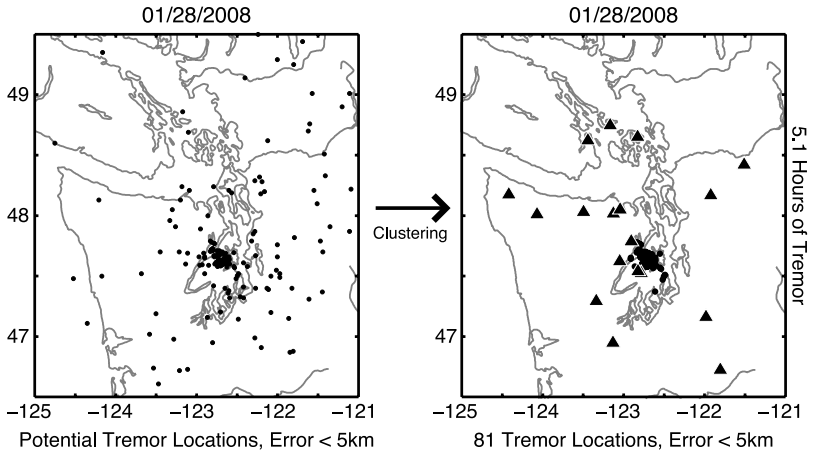

Figure 2. Example of detection on January 28, 2008. From all (left) preliminary locations with error estimates <5 km, only those with at least two epicenters in a 0.1 × 0.1 degree bin are kept as (right) final tremor epicenters. Station distribution is shown in Figure 2 (right).

obtain locations for every 50%-overlapping 5-minute window before determining its classification as tremor. Using bootstrap error estimates, only those solutions with epicentral error estimates less than 5 km are kept as potential tremor sources. We analyze these potential locations for clustering, requiring that at least 2 locations occur within a 0.1 × 0.1 degree area per day (Figure 2). These simple constraints, fine-tuned through trial and error, remove most random noise while adhering to one fundamental tremor definition—an enduring correlated signal localized in space [*Obara*, 2002].

[11] We test our detection ability by comparing our total daily tremor durations against analyst estimations over a period of 17 months spanning two ETS events (Figure 3). The strong agreement demonstrates the algorithm's ability to detect major ETS episodes as well as the many minor inter-ETS tremor bursts with no detectable geodetic signatures. Visual detection uses a subset of our autodetection envelopes, but the comparison's scale discrepancy may reflect the fact that manual methods require only two similar waveforms compared with three required by autolocation, making automation more susceptible to noisy stations. Hourly analysis of autodetected ETS tremor reveals a strong cultural signal with 8 hours of decreased daytime detection, which may contribute to our consistent detection of 2/3 manual estimations.

5. Comparison with Other Methods

[12] Our method is based on the method used in our previous studies [e.g., *Wech and Creager*, 2007] (the difference being an improved weighting scheme and automation facilitated by bootstrapping and clustering analysis) and is just one among many techniques for locating and detecting

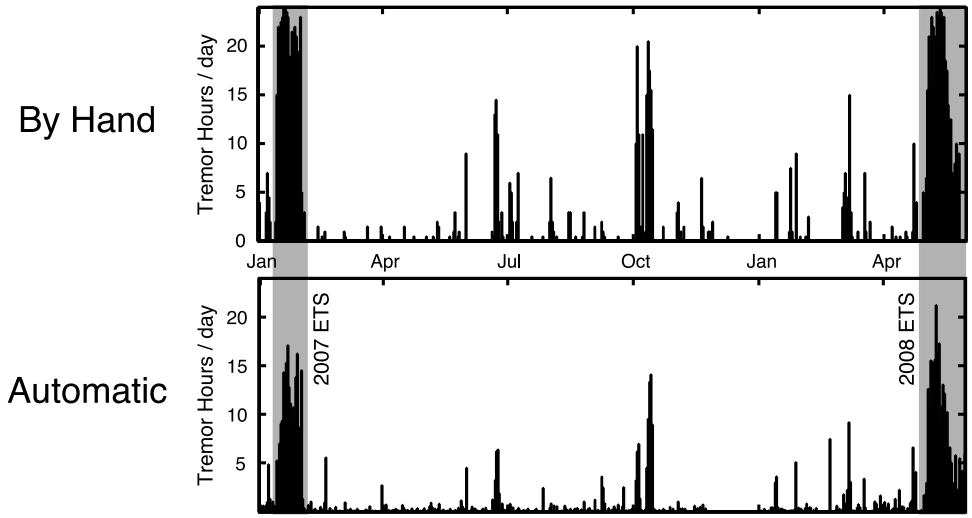

Figure 3. A comparison of daily tremor detection (top) by hand and (bottom) by our automated algorithm spanning from January 1, 2007–June 1, 2008. Grey regions show ETS episodes. From late November 2007 through early January 2008 there is a data gap for the automatic detections and a partial gap for the hand detections.

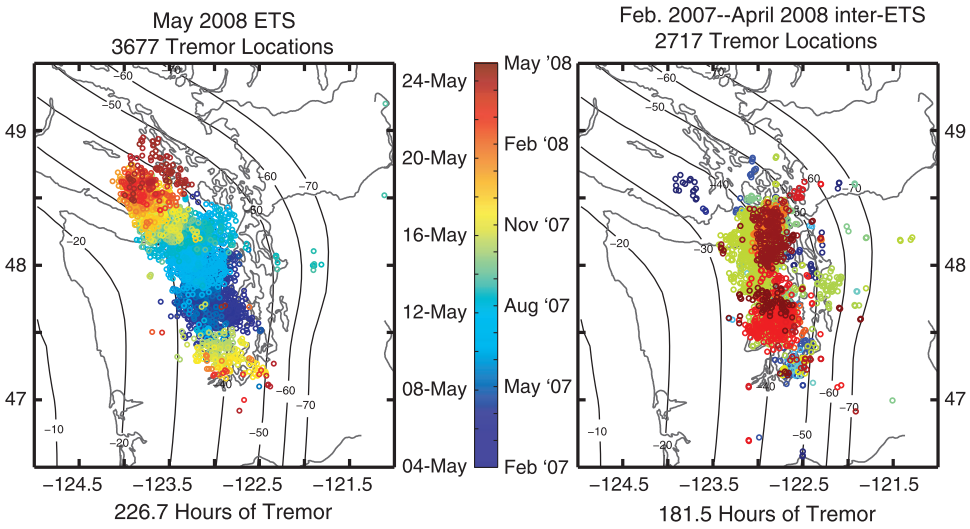

Figure 4. (left) May 2008 ETS and (right) February 2007–April 2008 inter-ETS tremor epicenters with error estimates <5 km separately color-coded by time. Contours show the plate interface depths [*McCrory et al.*, 2004]. For the May ETS episode, tremor continued an additional week under Vancouver Island, but our station distribution does not extend far enough north to capture it (Figure 4 (left)).

tectonic tremor. Starting with *Obara*'s, [2002] seminal tremor study, nearly every location method applies a band-pass filter to seismic data, rectifies with absolute values or envelopes and smoothes the envelopes. Obara estimates differential S-wave times between pairs of high-quality bore-hole seismometers from correlations of 1-minute-long envelope functions. He locates tremor from these times and then averages the locations obtained for each hour [*Obara*, 2002]. While our method is similar, we bootstrap to obtain error estimates on a much smaller time scale and diverge from this and all other methods by considering the correlation functions themselves to be the data. This provides some statistical advantages by handling correlation cycle skipping issues automatically and simply.

[13] Compared with the other techniques used currently in Cascadia, our location method is more easily incorporated into a routine monitoring system. First, it does not require small aperture arrays [*La Rocca et al.*, 2008; *McCausland*, 2006], but instead utilizes real-time regional data. Second, its ability to autolocate 1 day of tremor in 1 hour on a desktop computer makes it much less computationally intensive than *Kao and Shan*'s [2004] source-scanning algorithm. Finally, user-free automation makes it much less labor intensive than *McCausland et al.*'s [2005] method of picking features of envelope functions, allowing us to create a complete catalog in near-real time. As with the other Cascadia location methods, our tremor depths are widely scattered [*Kao et al.*, 2005; *McCausland et al.*, 2005], but with large uncertainties. Nevertheless, combining this method's epicenters with new tremor S-P time estimates (M. La Rocca, Array analysis and precise source location of deep tremor in Cascadia, submitted to *Journal of Geophysical Research*, 2008) could provide accurate hypocentral constraints.

[14] Our automatic detection algorithm is unique in that we focus on the locations of coherent signals seen across the network. Whereas *Kao et al.* [2005] focuses on characterizing patterns in signals among nearby stations, and *Brudzinski and Allen* [2007] examine mean envelope amplitudes at single stations, we analyze network coherence through epicentral reliability and spatial repeatability. Our method has the advantage of simultaneous location but may be less effective with just an hour-long time window and is unable to detect tremor from a single station time series [*Brudzinski and Allen*, 2007], requiring at least 3 but typically using 10–15 stations. Nevertheless, all three detection methods are capable of reproducing hand efforts [*Kao et al.*, 2007; *Brudzinski and Allen*, 2007] (Figure 3), rendering them effective at monitoring temporal behavior. The real strength in our method is providing simultaneous detection and location information, and its computationally frugal and simple nature makes it portable and easy to implement in other regions and on other networks.

6. Results

[15] We have applied our method to 17 months of data spanning two ETS episodes. The resulting 2,717 epicenters from the February 2007–April 2008 inter-ETS period and 3,677 epicenters from the May 2008 ETS (Figure 4) reveal two things. First, they chart the migration of the May 2008 ETS event with unprecedented detail. Color-coding epicenters by time shows 227 hours of tremor migrating from central Puget Sound to Vancouver Island from May 4th–24th and then north beyond our network's border, with a late burst occurring in southern Puget Sound on May 15th–17th (Figure 4). The epicenters occur in the mapped slow-slip region [*Szeliga et al.*, 2008], where the plate interface is 30–45 km deep. The epicenters have a well-resolved sharp updip boundary about 75 km east of current estimates of the downdip edge of the locked zone [*McCaffrey et al.*, 2007] (Figure 4). Second, during the 15 months between ETS episodes, we identify and locate numerous innocuous tremor bursts (Figure 3). Looking at days with more than 1 hour detected to avoid noise and earthquakes, we obtain

182 hours of inter-ETS tremor (Figure 4), which accounts for 45% of the tremor detected during the entire ETS cycle.

7. Implications

[16] Using tremor as a proxy for slow slip [*Hiramatsu et al.*, 2008; A. C. Aguiar et al., Moment rate during Cascadia tremor constrained by GPS, submitted to *Journal of Geophysical Research*, 2008.], our algorithm may provide a detailed map of the slow slip region, seismically identifying when, where, and how much slip is occurring. These capabilities are invaluable for investigating hazard potential and studying the tectonic processes involved. The discovery of 45% of geodetically undetectable tremor activity emphasizes the need for both spatial and temporal monitoring while requiring a new perspective on ETS dynamics. The narrowing distinction between tremor and slip combined with our inter-ETS totals and locations (Figure 4) suggests that the plates, thought to be coupled between ETS episodes, may accommodate the remaining plate convergence with no moment accumulation [*Dragert et al.*, 2001; *Szeliga et al.*, 2008] by exhibiting multiple episodes of slip (Figures 3 and 4) below GPS resolution. (A. G. Wech et al., Seismic and geodetic constraints on Cascadia slow slip, submitted to *Journal of Geophysical Research*, 2008). ETS and inter-ETS tremor epicenters have a sharp updip edge whose combined duration totals could account for nearly all of the plate convergence, suggesting that ETS occurs in the freely slipping zone with tremor epicenters demarcating the downdip edge of the margin's transition zone. This raises the important question: How is slip accommodated between the updip edge of ETS and the down-dip edge of the megathrust estimated near the coast? A megathrust rupture continuing to the updip edge of the ETS zone decreases the distance between the fault and major population centers by 50% from previous estimates [*McCaffrey et al.*, 2007].

[17] This example demonstrates our method's ability to track tremor spatially and temporally while highlighting the need for such capabilities both for monitoring and future research purposes. As observations of tremor expand to various tectonic settings around the world, the simplicity and portability of our automatic location and detection algorithm addresses the need for routine spatial and temporal monitoring while providing a handle for the abundant unanswered ETS questions.

[18] **Acknowledgments.** This material is based on work supported by the National Science Foundation and the USGS. Primary data were supplied by PNSN, PGC, Earthscope and PBO seismometers. We thank Robert Crosson for his envelope processing and Jenny Hanna for visually cataloging tremor. We also thank John Vidale, Weston Thelen, and Justin Sweet for valuable discussion.

References

Brudzinski, M. R., and R. M. Allen (2007), Segmentation in episodic tremor and slip all along Cascadia, *Geology*, *35*, 907–910, doi:10.1130/G23740A.1.

Dragert, H., K. Wang, and T. S. James (2001), A silent slip event on the deeper Cascadia subduction interface, *Science*, *292*, 1525–1528, doi:10.1126/science.1060152.

Efron, B. (1979), Bootstrap methods: Another look at the jackknife, *Ann. Stat.*, *7*, 1–26.

Hiramatsu, Y., T. Watanabe, and K. Obara (2008), Deep low-frequency tremors as a proxy for slip monitoring at plate interface, *Geophys. Res. Lett.*, *35*, L13304, doi:10.1029/2008GL034342.

Kao, H., and S.-J. Shan (2004), The source-scanning algorithm: Mapping the distribution of seismic sources in time and space, *Geophys. J. Int.*, *157*, 589–594.

Kao, H., S. Shan, H. Dragert, G. Rogers, J. F. Cassidy, and K. Ramachandran (2005), A wide depth distribution of seismic tremors along the northern Cascadia margin, *Nature*, *436*, 841–844, doi:10.1038/nature03903.

Kao, H., P. J. Thompson, G. Rogers, H. Dragert, and G. Spence (2007), Automatic detection and characterization of seismic tremors in northern Cascadia, *Geophys. Res. Lett.*, *34*, L16313, doi:10.1029/2007GL030822.

La Rocca, M., D. Galluzzo, S. Malone, W. McCausland, G. Saccorotti, and E. Del Pezzo (2008), Testing small-aperture array analysis on well-located earthquakes, and application to the location of deep tremor, *Bull. Seismol. Soc. Am.*, *98*, 620–635.

McCaffrey, R., A. I. Qamar, R. W. King, R. Wells, G. Khazaradze, C. A. Williams, C. W. Stevens, J. J. Vollick, and P. C. Zwick (2007), Fault locking, block rotation and crustal deformation in the Pacific Northwest, *Geophys. J. Int.*, *169*, 1315–1340.

McCausland, W. (2006), Tracking subduction tremor in Cascadia using regional network and small-aperture seismic array data, Ph.D. dissertation, Univ. of Wash., Seattle.

McCausland, W., S. Malone, and D. Johnson (2005), Temporal and spatial occurrence of deep non-volcanic tremor: From Washington to northern California, *Geophys. Res. Lett.*, *32*, L24311, doi:10.1029/2005GL024349.

McCrory, P. A., J. L. Blair, D. H. Oppenheimer, and S. R. Walter (2004), Depth to the Juan de Fuca slab beneath the Cascadia subduction margin-A 3-D model for sorting earthquakes, *U.S. Geol. Surv. Data Ser.*, *91*.

Obara, K. (2002), Nonvolcanic deep tremor associated with subduction in southwest Japan, *Science*, *296*, 1679–1681.

Obara, K., H. Hirose, F. Yamamizu, and K. Kasahara (2004), Episodic slow slip events accompanied by non-volcanic tremors in southwest Japan subduction zone, *Geophys. Res. Lett.*, *31*, L23602, doi:10.1029/2004GL020848.

Rogers, G., and H. Dragert (2003), Episodic tremor and slip on the Cascadia subduction zone: The chatter of silent slip, *Science*, *300*, 1942–1943, doi:10.1126/science.1084783.

Shelly, D. R., G. C. Beroza, and S. Ide (2007), Non-volcanic tremor and low-frequency earthquake swarms, *Nature*, *446*, 305–307, doi:10.1038/nature05666.

Szeliga, W., T. Melbourne, M. Santillan, and M. Miller (2008), GPS constraints on 34 slow slip events within the Cascadia subduction zone, 1997–2005, *J. Geophys. Res.*, *113*, B04404, doi:10.1029/2007JB004948.

Wech, A. G., and K. C. Creager (2007), Cascadia tremor polarization evidence for plate interface slip, *Geophys. Res. Lett.*, *34*, L22306, doi:10.1029/2007GL031167.

K. C. Creager and A. G. Wech, Department of Earth and Space Sciences, University of Washington, Box 351310, Seattle, WA 98195, USA. (wech@u.washington.edu)